Achieving High Field-Effect Mobility in Amorphous Indium-Gallium-Zinc Oxide by Capping a Strong Reduction Layer

Hsiao-Wen Zan, Chun-Cheng Yeh, Hsin-Fei Meng, Chuang-Chuang Tsai, and Liang-Hao Chen*

Transparent oxide semiconductors (TOSs) have been intensively studied in the past decade because they have a wide variety in material properties. The conductivity can be tuned from conducting to insulating by changing the cation composition and the oxygen vacancy concentration.[1] Ferromagnetic and ferroelectric behaviors observed in doped ZnO can be used to develop new spin-tronics devices and advanced data storage.[2] Ultraviolet lasing from ZnO nanowires (NWs) opens a promising route to construct transparent optoelectronics.[3] TOS-based transistors, including nanowire field-effect transistors (NW FETs) and thin-film transistors (TFTs), also have drawn lots of attention because they possess high electron mobility at low process temperature.[4,5] Particularly, for TOSs containing heavy metal cations, electron conduction paths are formed by the spatially spread metal s-orbitals with an isotropic shape and electron mobility is insensitive to the distorted metal-oxygen-metal bonds.[5] Thus, amorphous oxide semiconductor (AOS) thin films exhibits an electron mobility higher than 10 $cm^2V^{-1}s^{-1}$, which is substantially higher than the electron mobility of amorphous silicon.

Instead of metal-oxygen bonding system, the defects associated with oxygen deficiencies are reported to cause electron scattering, electron trapping, and reduced electron mobility in ZnO NW FETs.[6] Passivating surface defects on single crystal ZnO nanorods with polyimide coating or SiO_2/Si_3N_4 bilayer coating can significantly increase electron mobility by one to two orders compared to un-passivated samples.[7,8] In AOSs, electron mobility is also sensitive to defect states.[9] It is therefore expected to increase mobility significantly by reducing defect density. In this report, we firstly demonstrated a successful method to reduce defects and to increase electron mobility in an AOS thin-film transistor. We capped a calcium/aluminum dual layer onto the back interface of amorphous Indium-Gallium-Zinc Oxide (a-IGZO) TFTs. Right after Ca/Al evaporation, electron mobility increased from 12 $cm^2V^{-1}s^{-1}$ to 160 $cm^2V^{-1}s^{-1}$. This high mobility is a new state-of-the-art in AOSs, indicating that the proposed defect reduction effect is key to improve electron transport in oxide semiconductor materials.[10–13] Defect reduction effect is expected to be critical in handling electrical properties as well as optical properties and ferroelectric properties of TOSs because the variation of defect states also changes the sub-bandgap state distribution.[14–16]

Experimental results are introduced and discussed as follows: Firstly, the transfer characteristics of the proposed Ca/Al-capped a-IGZO TFT are demonstrated. The proposed device is tracked for 50 days to observe the time related behavior caused by the oxidation of capped calcium. Then, the defect reduction mechanism is investigated by using X-ray photoelectron spectroscope (XPS) depth profile analysis to characterize atomic distribution and chemical bonding of Ca/Al-capped a-IGZO film. Devices with different a-IGZO thicknesses are compared. Bias-stress reliability is discussed. Finally, high electron mobility in a silicon-capped a-IGZO TFT is shown to support the proposed defect reduction mechanism.

The structure of the Ca/Al-capped a-IGZO TFT is shown in **Figure 1**a. The Ca/Al capping layer (with a length as 150 μm) covers central 50% area of the channel region (channel length is 300 μm). The transfer characteristics of the Ca/Al-capped device and the standard (STD) device are shown in Figure 1b. After Ca/Al capping, the field-effect mobility increased from 12.1 $cm^2V^{-1}s^{-1}$ to 160 $cm^2V^{-1}s^{-1}$. The threshold voltage, V_T, of the Ca/Al-capped device shifted from 1.4 V to –25 V. In our previous work, the threshold voltage shift of the Ca/Al-capped device was investigated.[17] The shift in threshold voltage can be explained by the electron injection from Ca into a-IGZO because of the work function difference. A negative gate bias is needed to deplete the active layer and to turn off the device. In our previous work, we didn't observe the significant increase in electron mobility in the Ca/Al-capped device. In this work, we performed 30-min pre-evaporation before evaporating Ca onto a-IGZO film. A significantly increased mobility was obtained. This suggests that the pure Ca evaporated onto a-IGZO is critical to initiate reactions between Ca and a-IGZO and to obtain the high mobility.

The high electron mobility may be caused by the reduction of defect density inside a-IGZO film. For a-IGZO, electron mobility is governed by percolation conduction model with potential barriers above mobility edges. The potential barriers are dependent on atomic structure and disorder network of a-IGZO film.[18] Reducing defects in a-IGZO film may decrease the potential barrier and increase mobility. Defects in a-IGZO are various kinds of oxygen-vacancy defects.[19] The diffusion of calcium into a-IGZO film and the oxidation of these calcium

Prof. H.-W. Zan, C.-C. Yeh, Prof. C.-C. Tsai, L.-H. Chen
Department of Photonics and Institute of Electro-Optical Engineering
National Chiao Tung University
1001, Ta-Hsueh Rd, HsinChu, 300, Taiwan
E-mail: hsiaowen@mail.nctu.edu.tw
Prof. H. F. Meng
Institute of Physics
National Chiao Tung University
1001, Ta-Hsueh Rd, HsinChu, 300, Taiwan

DOI: 10.1002/adma.201200683

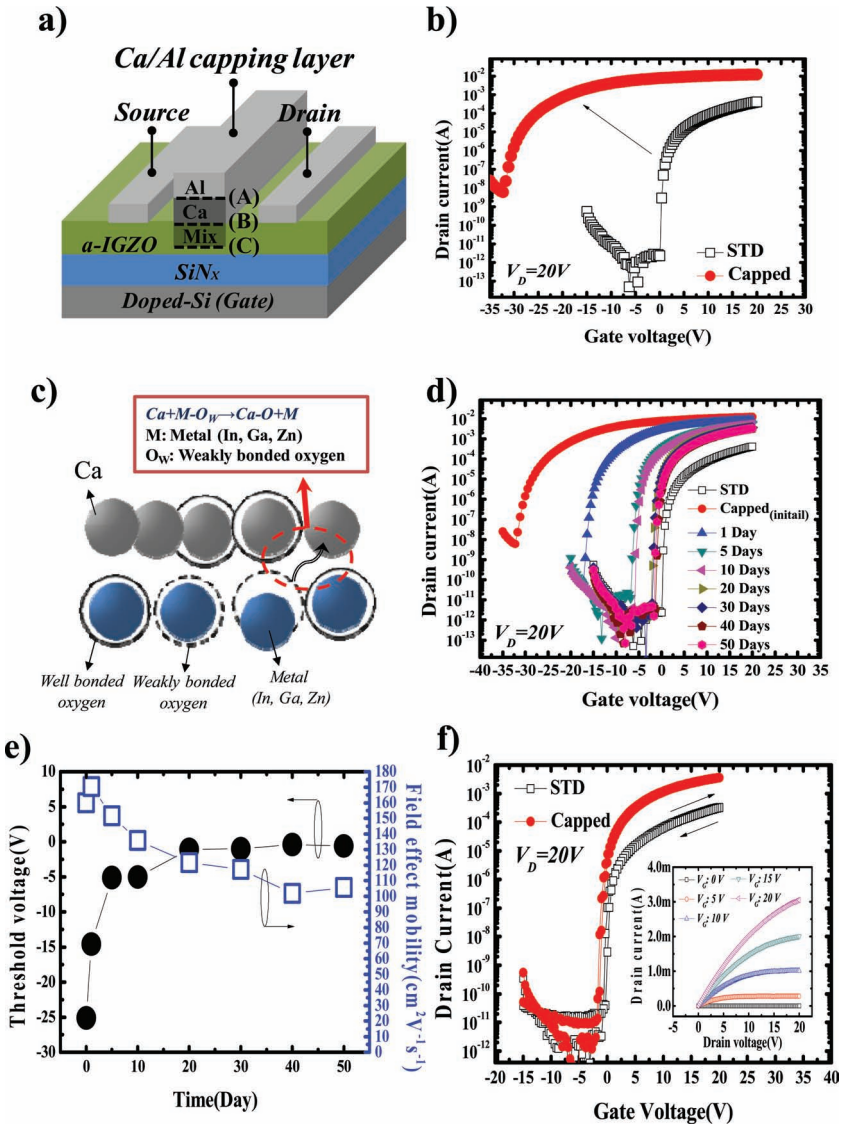

Figure 1. (a) Bottom-gate top-contact a-IGZO TFT (STD device) is capped with Ca/Al dual layer. The Ca/Al capping layer (with a length as 150 μm) covers central 50% area of the channel region (channel length is 300 μm). (b) The transfer characteristics of STD and of Ca/Al-capped a-IGZO TFTs. (c) Weakly bonded oxygen atoms change their bindings to nearby calcium and form calcium oxide. (d) Transfer characteristics of STD and Ca/Al capped a-IGZO TFT during 50 days stored in air. (e) The variation of threshold voltage and mobility for Ca/Al-capped device during 50 days stored in air. (f) The hysteresis of STD and of stabilized Ca/Al-capped a-IGZO TFT. The inset shows the output characteristics of stabilized Ca/Al capped a-IGZO TFT.

atoms inside a-IGZO film may reduce the concentration of weakly bonded oxygen as well as the defect density inside a-IGZO film for its high reducing power. (Figure 1c) Therefore, significantly enhanced electron mobility is obtained.[7,8]

After the Ca/Al-capped device is exposed to air, its transfer characteristics exhibit a time decay behavior as shown in Figure 1d. The transfer characteristics of the STD device are also plotted in Figure 1d for reference. The mobility and threshold voltage of the Ca/Al-capped device as a function of exposure time are shown in Figure 1e. The threshold voltage of the Ca/Al-capped device recovered rapidly after exposing to air, it stabilized after 20-days in air. The stabilized threshold voltage around 0 V is close to that of the uncapped device (1.4 V). The mobility of the Ca/Al capped device also dropped after exposure to air, but stabilized after 40 days. The stabilized mobility is a 100 $cm^2V^{-1}s^{-1}$ and is still much higher than that of the uncapped device, 12 $cm^2V^{-1}s^{-1}$. Detailed parameters are listed in **Table 1**. Threshold voltage and mobility are extracted from the slope and the x-axis intercept of the $\sqrt{I_D}$–V_{GS} curve measured under saturation condition.[16] The output characteristic of stabled Ca/Al-capped device is shown in the inset of Figure 1f. The hysteresis effects of the stabilized Ca/Al-capped device and STD device were checked as shown in Figure 1f, and no hysteresis was observed for either device.

As mentioned, the threshold voltage shift is due to electron injection from Ca into a-IGZO because the work function of Ca is lower than the conduction band of a-IGZO. The recovery of threshold voltage shift is plausible because Ca is oxidized easily in air. In our experiment, Ca is capped by Al; thus, the Ca oxidation was postponed and the threshold voltage took 20 days to stabilize.

A defect reduction effect is proposed to explain the significantly increased mobility and its slow stabilization of mobility in Ca/Al-capped devices. Calcium has strong reducing power and small atom size. When pure Ca is capped onto a clean a-IGZO surface, Ca atoms may diffuse into a-IGZO film quickly. The abundant oxygen atoms inside a-IGZO react with Ca easily. At the same time, some weakly-bonded oxygen atoms in non-perfect Zn-O, In-O, and Ga-O bonds may also escape from their original bonds to form Ca-O bonds. This process leads to a decrease of weakly bonded oxygen density, as well as to a reduction in the defect density inside a-IGZO film. After Ca/Al-capped devices exposed to air, the abundant oxygen in air may join this reaction and affect the equilibrium between Zn-O, In-O, Ga-O, Ca-O and oxygen deficiencies. The complicated interaction among all these elements and bonds make it difficult and slow to reach equilibrium. Hence, the stabilization of mobility is slow.

X-ray photoelectron spectroscope (XPS) analysis is used to characterize the atomic distribution and the chemical bonding of a Ca/Al-capped a-IGZO film. Firstly, the depth profile of atomic concentration of the structure Al/Ca/a-IGZO (100 nm/35 nm/100 nm) on silicon substrate with thermal grown SiN_x is investigated. The Ar sputtering etching rate for a-IGZO was approximately 7 nm/min. **Figure 2**a shows the element content variation while etching from the top of the sample, and the (A), (B), and (C) symbols on top of the figure correspond to the position labeled by the same symbols in Figure 1a. From

Table 1. Extracted parameters of Ca/Al-capped a-IGZO TFT traced during 50 days stored in air. V_T, μ_{FE}, and S.S. are threshold voltage, field-effect mobility and subthreshold swing, respectively. Parameters of the STD device are also listed for comparison.

Ca/Al capped	Time [days]	V_T [V]	μ_{FE} [$cm^2 V^{-1} s^{-1}$]	S.S. [V decade^{-1}]	On/Off ratio
	0	−25.1	160	0.76	2.9×10^6
	1	−14.6	170.4	0.44	1.5×10^8
	5	−5.1	151.6	0.23	4.5×10^8
	10	−5	135.8	0.2	1.2×10^9
	20	−1.1	121.7	0.17	9.7×10^8
	30	−1	117.2	0.13	5.5×10^8
	40	−0.4	101.9	0.14	9.2×10^8
	50	−0.6	105.7	0.12	9.7×10^8
STD	–	1.4	12.1	0.11	1.8×10^8

Figure 2a, we can obviously observe the diffusion of Ca into a-IGZO film with a diffusion depth around 20 nm. A mixed layer containing both a-IGZO and Ca is formed on top of the a-IGZO film. We extract the binding energies for all elements (Ca, O, In, Ga, Zn) of the Ca/Al-capped a-IGZO sample with various depths to examine the Ca effect in detail. We first check the binding energy of Ca as shown in Figure 2b. The double peaks, 346.7 eV and 352.3 eV, are attributed to the ionization of the two fine structures, Ca $2p^3$ and Ca $2p^1$.[20] No peak shift was observed when changing the depth position inside a-IGZO film, indicating a complete oxidation of Ca inside the a-IGZO film and the formation of a-IGZCaO alloy. Figure 2c shows the binding energy variations of O 1s orbital, and the signal from a bare a-IGZO film is plotted for comparison. When the sputtering time is 11 mins, a-IGZO film is doped with a very low Ca concentration (<2%). The O 1s binding energy is almost identical to that of a bare a-IGZO. When the sputtering time is 8 min, the depth position is close to the surface of the a-IGZO film and Ca concentration is high (15.2%). The photoelectron peak of O 1s orbital is 0.4 eV lower than that of a bare a-IGZO film. It is known that, for O 1s orbital, the peak energy at 529.5 ± 0.5 eV refers to well bonded oxygen, whereas the peak energy at 531 ± 0.5 eV refers to oxygen associated lattice defects such as oxygen vacancies, metal vacancies and/or interstitials adjacent to the oxygen in the lattice structure.[21,22] Our experimental results reveal that doping a-IGZO with Ca improves the oxygen bonding in a-IGZO film.

The binding energies for Zn, In, and Ga with various depths are shown in Figures 2d, 2e, and 2f, respectively. For these three elements, a significant left shift of the peak energy is observed near the a-IGZO surface with a high Ca concentration. The oxidized states, or ionized states, of the three compounds ZnO, InO, and GaO exhibit higher binding energy than Zn, In, and Ga.[23–25] The decrease of binding energy near the capping layer reveals that the oxidation states of Zn, In, and Ga are decreased. The electronegativity of Ca (0.95) is lower than that for Zn (1.65), Ga (1.81), and In (1.78). Therefore, the oxygen-binding ability of Ca is higher than that of Zn, Ga, and In. Some weakly bonded

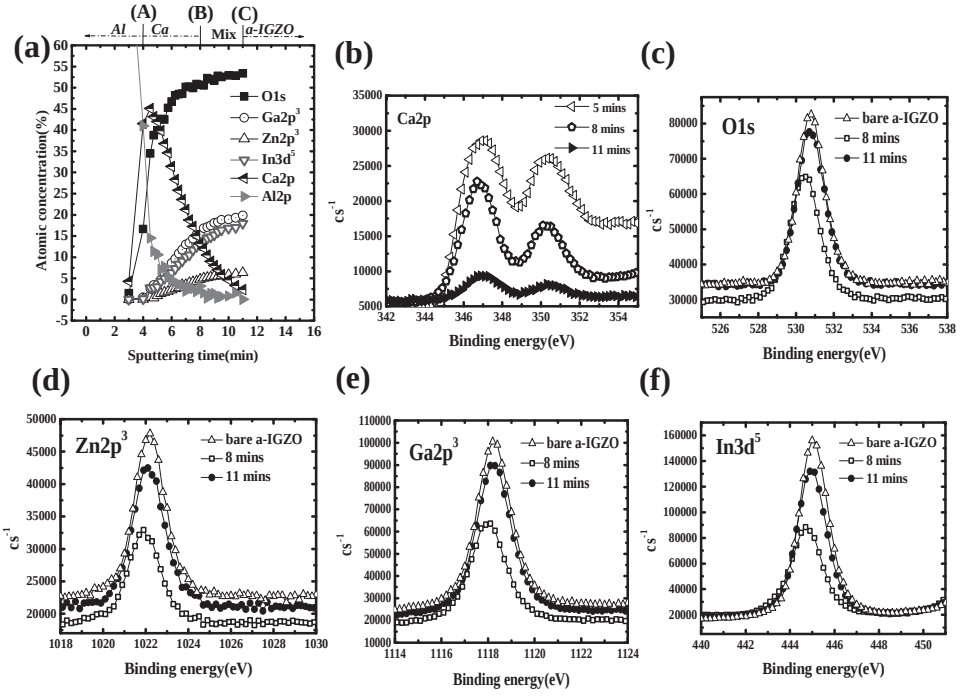

Figure 2. (a) XPS depth profile of various elements in Ca/Al-capped a-IGZO sample. Position (A) and (B) indicate the Al/Ca interface and the surface of a-IGZO. A mixing layer contains Ca and a-IGZO exists from (B) to (C). (b) Ca 2p XPS binding energy spectra in Ca capped layer (5 min), on top of the mixing layer (8 min) and on bottom of the mixing layer (11 min). (c) O 1s (d) Zn $2p^3$ (e) Ga $2p^3$ and (f) In $3d^5$ XPS binding energy spectra in bare a-IGZO and in Ca/Al capped sample. 8 and 11 min indicate the top and bottom positions of the mixing layer.

oxygen atoms in Zn-O, In-O, and Ga-O bonds may escape from their original bonds to form Ca-O bonds leading to the reduction of binding energies of Zn, In, and Ga in the a-IGZO film near the capping layer. The removal of weakly bonded oxygen in Zn-O, In-O, and Ga-O bonds agree well with the results shown Figure 2c. The incorporation of Ca into a-IGZO improves the oxygen bonding and reduces the defect density.

To gain a more in-depth understanding of the Ca/Al-capped device, we changed the thickness of the a-IGZO film from 50 nm, 35 nm to 15 nm. The transfer characteristics of STD (uncapped) devices with an IGZO thickness of 50 nm, 35 nm, and 15 nm are shown in **Figure 3**a. No significant difference was observed. When devices were capped by Ca/Al layer, the transfer characteristics of these three devices are compared in Figure 3b. The initial characteristics right after capping and the stabilized characteristics are plotted. For device with 15-nm-thick or 35-nm-thick a-IGZO, after stabilization, threshold voltage recovered back to around 0 V. For device with 50-nm-thick

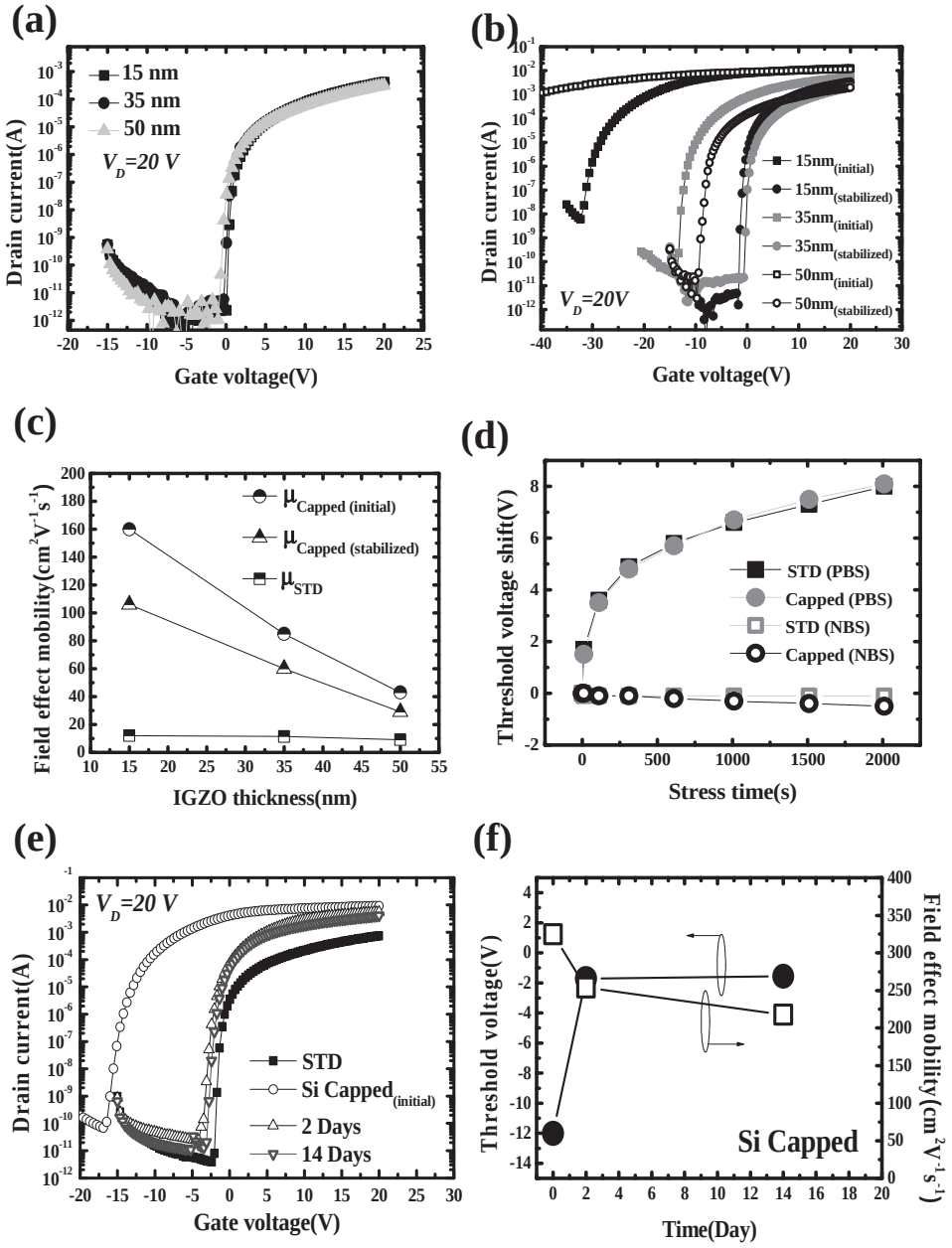

Figure 3. (a) The transfer characteristics of STD with various a-IGZO thicknesses. (b) The initial (as-capping) and stable transfer characteristics of Ca/Al-capped a-IGZO TFTs with various a-IGZO thicknesses. (c) Field-effect mobility as a function of a-IGZO thicknesses for STD and Ca/Al-capped devices. (d) The comparison of threshold voltage shifts of Ca/Al capped and STD a-IGZO TFT under 2000s PBS and NBS as a function of stress duration time. (e) Transfer characteristics of STD and Si-capped a-IGZO TFT. Si-capped device are traced for 14 days in air. (f) Threshold voltage and mobility for Si capped a-IGZO TFT (stored in air) are plotted as a function of traced time.

a-IGZO, on the contrary, a negatively shift threshold voltage is obtained even after stabilization. The reason is still unknown. The mobilities of these three devices are compared in Figure 3c. A clear trend can be obtained that the thicker IGZO film gives rise to the smaller mobility. In Figure 2a, it is found that the Ca diffusion depth is around 20 nm. The defect reduction effect is limited near the Ca capping layer. For a bottom gate a-IGZO TFT, carriers flow close to the bottom interface of IGZO. When increasing the IGZO thickness, the defect reduction effect becomes inferior near the bottom of IGZO and thus the mobility enhancement is less significant.

To evaluate the reliability of the stabled Ca/Al-capped device, a bias stress experiment is performed. The bias stress conditions are $V_{GS} - V_T = +20$ V for positive bias stress (PBS), and $V_{GS} - V_T = -20$ V for negative bias stress (NBS), with drain bias $V_{DS} = 0$ V during stress. No significant difference can be found between capped and STD devices. (Figure 3d) In our work, standard (without Ca/Al) a-IGZO TFT and Ca/Al-capped a-IGZO TFT do not have passivation layers. Amorphous a-IGZO TFT without passivation was reported to exhibit large positive-bias-stress-induced threshold voltage shift due to the interaction between ambient oxygen/water and a-IGZO film.[26] The results in Figure 3d reveal that the incorporation of Ca into a-IGZO does not lead to enhanced interaction between ambient and a-IGZO film during bias stress. Adding passivation layer onto the Ca/Al-capped a-IGZO TFTs is expected to improve the bias-stress reliability of Ca/Al-capped a-IGZO TFT.[26,27] Finally, in addition to Ca capping, another material with high reducing power, silicon (Si), was capped onto a-IGZO TFT. The transfer characteristics of the a-IGZO TFT measured before capping, right after Si capping (initial), 2-days and 14-days after Si capping are shown in Figure 3e. The mobility and threshold voltage plotted as a function of time after capping (and exposing to air) are in Figure 3f. A mobility as high as 217.5 cm^2/Vs is obtained for the Si-capped device stabilized after 14 days in air. More detailed investigations are ongoing. The very high mobility in Si capped device, however, supports the defect reduction effect proposed in this study.

In addition to the defect reduction effect, the incorporation of Ca into a-IGZO may also increase the material bandgap and then cause a graded band structure in vertical direction. In a crystalline MgZnO/ZnO heterojunction system, high electron mobility is obtained due to the formation of two dimensional electron gas. In our experiment, it is believed that high mobility is dominated by the defect reduction effect. The influence of a graded heterojunction band structure on electron mobility, however, is also discussed in the supporting information.

In summary, we use a strong reduction capping layer (calcium/aluminum dual layer, Ca/Al) to cap the back interface of conventional bottom-gate top-contact a-IGZO TFTs. The field-effect mobility increases from 12 $cm^2V^{-1}s^{-1}$ (uncapped standard device) to 160 $cm^2V^{-1}s^{-1}$ right after capping and is stabilized at 100 $cm^2V^{-1}s^{-1}$ after being stored 40 days in air. XPS depth profile analysis was conducted to investigate the atomic concentration profiles and the binding energy variations after Ca/Al capping. It is observed that calcium atoms diffuse into a-IGZO film with a diffusion depth around 20 nm. Inside a-IGZO film, particularly close to the IGZO/Ca interface, calcium atoms are oxidized to form CaO. Binding-energy peaks of oxygen, In, Zn, and Ga show a left shift close to the IGZO/Ca interface, suggesting that weakly bonded oxygen atoms in Zn-O, In-O, and Ga-O bonds may escape from their original bonds to form Ca-O bonds. The removal of weakly bonded oxygen in Zn-O, In-O, and Ga-O bonds improves the oxygen bonding, reduces the defect density, and enhances electron mobility. In addition to Ca/Al, we also capped Si onto the back interface of a-IGZO TFT and obtaining a field-effect mobility higher than 200 $cm^2V^{-1}s^{-1}$. The high mobility in this work is a new state-of-the-art record in AOSs, indicating that the proposed defect reduction effect is key to success in handling oxide semiconductor materials.

Experimental Section

A 100-nm-thick layer of thermal silicon nitride (SiN_x) was grown on doped Si wafers to serve as the gate dielectric. A thin 15-nm-thick layer of *a*-IGZO (3-in circular target: In:Ga:Zn = 1:1:1 at%) was deposited by radio-frequency (RF) sputtering onto thermally grown SiN_x through a shadow mask to form the active layer at room temperature. The RF power and pressure were 100 W and 9 mtorr, respectively. The introduced gas is argon with a constant flow rate of 30 sccm. The annealing process at 350 °C was conducted in a nitrogen furnace for 1 h. As shown at Figure 1a, a bottom-gate top-contact a-IGZO TFT (STD device) was completed after a 50-nm-thick layer of aluminum (Al) was deposited through a shadow mask to form the source and drain contacts. The channel width and length are 1000 μm and 300 μm, respectively. Then, the 150-μm-long, 35 nm thick Ca layer was deposited on the back channel of some STD devices to serve as the mobility-enhancement capping layer. To control the Ca film quality, a 30 min pre-evaporation was needed before evaporating Ca onto a-IGZO film. Finally, a 100-nm-thick Al was deposited on the Ca layer in sequence to prevent the formation of CaO, $Ca(OH)_2$ and $CaCO_3$ by absorbing oxygen, water and carbon dioxide from the atmosphere. The reaction between Ca and atmosphere was found to suppress the reaction between Ca and a-IGZO film.

Supporting Information

Supporting Information is available from the Wiley Online Library or from the author.

Acknowledgements

This work was supported by E Ink Holdings Inc. and the National Science Council of Taiwan under Contract No. NSC 100-2628-E-009-018-MY3.

Received: February 16, 2012
Revised: April 3, 2012
Published online: June 8, 2012

[1] S. Jeong, Y. G. Ha, J. Moon, A. Facchetti, T. J. Marks, *Adv. Mater.* **2010**, *22*, 1346.
[2] T. S. Herng, M. F. Wong, D. C. Qi, J. B. Yi, A. Kumar, A. Huang, F. C. Kartawidjaja, S. Smadici, P. Abbamonte, C. Sanchez-Hanke, S. Shannigrahi, J. M. Xue, J. Wang, Y. P. Feng, A. Rusydi, K. Y. Zeng, J. Ding, *Adv. Mater.* **2011**, *23*, 1635.
[3] J. Elias, C. Lévy-Clément, M. Bechelany, J. Michler, G. Y. Wang, Z. Wang, L. Philippe, *Adv. Mater.* **2010**, *22*, 1607.
[4] Eric N. Dattoli, Qing Wan, Wei Guo, Yanbin Chen, Xiaoqing Pan, Wei Lu, *Nano Lett.* **2007**, *7*, 2463.

[5] K. Nomura, H. Ohta, A. Takagi, T. Kamiya, M. Hirano, H. Hosono, *Nature* **2004**, *432*, 488.
[6] G. Eranna, B. C. Joshi, D. P. Runthala, R. P. Gupta, *Crit. Rev. Solid State Mater. Sci.* **2004**, *29*, 111.
[7] P. C. Chang, Z. Fan, C. J. Chien, D. Stichtenoth, C. Ronning, J. G. Lu, *Appl. Phys. Lett.* **2006**, *89*, 133113.
[8] W. I. Park, J. S. Kim, G. C. Yi, M. H. Bae, H. J. Lee, *Appl. Phys. Lett.* **2004**, *85*, 5052.
[9] J. H. Jeong, H. W. Yang, J. S. Park, J. K. Jeong, Y. G. Mo, H. D. Kim, J. Song, C. S. Hwang, *Electrochem. Solid-State Lett.* **2008**, *11*, H157.
[10] S.I. Kim, C. J. Kim, J. C. Park, I. Song, S. W. Kim, H. Yin, E. Lee, J. C. Lee, Y. Park, *IEDM* **2008**, *15–17*, 1.
[11] H. N. Lee, J. Kyung, M. C. Sung, D. Y. Kim, S. K. Kang, S. J. Kim, C. N. Kim, H. G. Kim, S. T. Kim, *J. Soc. Inf. Disp.* **2008**, *16*, 265.
[12] C. J. Chiu, S. P. Chang, S. J. Chang, *IEEE Electron Device Lett.* **2010**, 31, 1245.
[13] H. W. Zan, W. W. Tsai, C. C. Chen, C. C. Tsai, *Adv. Mater.* **2011**, *23*, 4237.
[14] B. Panigrahy, M. Aslam, D. S. Misra, M. Ghosh, D. Bahadur, *Adv. Funct. Mater.* **2010**, *20*, 1161.
[15] H. Seo, C. J. Park, Y. J. Cho, Y. B. Kim, D. K. Choi, *Appl. Phys. Lett.* **2010**, *96*, 232101.
[16] T. Kamiya, K. Nomura, H. Hosono, *Sci. Technol. Adv. Mater.* **2010**, *11*, 044305.
[17] H. W. Zan, W. T. Chen, C. C. Yeh, H. W. Hsueh, C. C. Tsai, H. F. Meng, *Appl. Phys. Lett.* **2011**, *98*, 153506.
[18] T. Kamiya, K. Nomura, H. Hosono, *J. Displays Technol.* **2009**, *5*, 462.
[19] H. K. Noh, K. J. Chang, B. Ryu, W. J. Lee, *Phys. Rev. B.* **2011**, *84*, 115205.
[20] D. Ochs, B. Braun, W. Maus-Friedrichs, V. Kempter, *Surf. Sci.* **1998**, *417*, 406.
[21] D. S. Shang, L. D. Chen, Q. Wang, W. D. Yu, X. M. Li, J. R. Sun, B. G. Shen, *J. Appl. Phys.* **2009**, *105*, 063511.
[22] N. Xu, L. Liu, X. Sun, X. Liu, D. Han, Y. Wang, R. Han, J. Kang, B. Yu, *Appl. Phys. Lett.* **2008**, *92*, 232112.
[23] D. Wett, A. Demund, H. Schmidt, R. Szargan, *Appl. Surf. Sci.* **2008**, *254*, 2309.
[24] R. W. Hewitt, N. Winograd, *J. Appl. Phys.* **1980**, *51*, 2620.
[25] S. J. Kerber, T. L. Barr, G. P. Mann, W. A. Brantley, E. Papazoglou, J. C. Mitchell, *J. Mater. Engng Perform.* **1998**, 7, 334.
[26] J. K. Jeong, H. W. Yang, J. H. Jeong, Y. G. Mo, H. D. Kim, *Appl. Phys. Lett.* **2008**, *93*, 123508.
[27] J. S. Lee, J. S. Park, Y. S. Pyo, D. B. Lee, E. H. Kim, D. Stryakhilev, T. W. Kim, D. U. Jin, Y. G. Mo, *Appl. Phys. Lett.* **2009**, *95*, 123502.